Journal of Magnetic Resonance 197 (2009) 181–185

Contents lists available at ScienceDirect

Journal of Magnetic Resonance

journal homepage: www.elsevier.com/locate/jmr

Pulsed EPR imaging of nitroxides in mice

Fuminori Hyodo [a,b,1], Shingo Matsumoto [a,*,1], Nallathamby Devasahayam [a], Christopher Dharmaraj [a], Sankaran Subramanian [a], James B. Mitchell [a], Murali C. Krishna [a]

[a] Radiation Biology Branch, Center for Cancer Research, National Cancer Institute, National Institutes of Health, 9000 Rockville Pike, Building 10, Room B3B69, Bethesda, MD 20892-1002, USA
[b] Innovation Center for Medical Redox Navigation, Kyushu University, Fukuoka, Japan

ARTICLE INFO

Article history:
Received 4 November 2008
Available online 24 December 2008

Keywords:
Nitroxide
Oximetry
Pulsed EPR
Redox
Single point imaging

ABSTRACT

Nitroxides, unlike trityl radicals, have shorter T_2s which until now were not detectable *in vivo* by a time-domain pulsed Electron Paramagnetic Resonance (EPR) spectrometer at 300 MHz since their phase memory times were shorter than the spectrometer recovery times. In the current version of the time-domain EPR spectrometer with improved spectrometer recovery times, the feasibility of detecting signals from nitroxide radicals was tested. Among the nitroxides evaluated, deuterated ^{15}N-Tempone (^{15}N-PDT) was found to have the longest T_2. The signal intensity profile as a function of concentration of these agents was evaluated and a biphasic behavior was observed; beyond a nitroxide concentration of 1.5 mM, signal intensity was found to decrease as a result of self-broadening. Imaging experiments were carried out with ^{15}N-PDT in solutions equilibrated with 0%, 5%, 10%, and 21% oxygen using the single point imaging (SPI) modality in EPR. The image intensity in these tubes was found to depend on the oxygen concentration which in turn influences the T_2 of ^{15}N-PDT. *In vivo* experiments were demonstrated with ^{15}N-PDT in anesthetized mice where the distribution and metabolism of ^{15}N-PDT could be monitored. This study, for the first time shows the capability to image a cell-permeable nitroxide in mice using pulsed EPR in the SPI modality.

1. Introduction

Nitroxides, also known as aminoxyls or nitroxyls, are stable free radicals that have unique antioxidant properties [1]. Undergoing reversible redox transformations between the three oxidation states of nitroxide, hydroxylamine, and the oxoammonium cation, nitroxides are able to mimic the catalytic activities of important antioxidant enzymes such as superoxide dismutase, catalase as well as participate in radical scavenging and H-atom donating reactions to provide stoichiometric antioxidant activities [2]. Discovery of many protective modes of nitroxides in *in vitro* and *in vivo* models of oxidative stress expanded the use of nitroxide to therapeutic applications, including protection against ionizing radiation, as cancer prevention and treatment, control of hypertension and weight, and protection from damage resulting from ischemia/reperfusion injury, etc. [2,3].

Up to now, three imaging techniques, continuous wave (CW) Electron Paramagnetic Resonance (EPR) imaging, conventional Magnetic Resonance Imaging (MRI), and Overhauser MRI (OMRI) have been used to monitor nitroxides in living objects [4–13]. The EPR imaging based on continuous wave (CW) approach is a direct method for imaging paramagnetic species with large line widths such as nitroxides [4,5], though it relatively takes long time for image data acquisition especially for 3D imaging. MRI provides anatomic image with superior spatial and temporal resolutions. Nitroxides have a single unpaired electron and can provide T_1 contrast to water protons in conventional MRI [7,12]. However, the molar relaxivity of nitroxides is $\sim$0.2 $mM^{-1}\,s^{-1}$ compared to 4.0 $mM^{-1}\,s^{-1}$ for Gd^{3+} complexes. In terms of contrast enhancement per unit volume, the lower relaxivity of nitroxides compared with Gd^{3+} complexes can be partially compensated by their large distribution volume due to small molecular size and cell-permeability of nitroxide [7]. In MRI, a fast Look-Locker T_1-mapping sequence, instead of typical dynamic T_1 weighted imaging, can quantify nitroxide levels *in vivo* [14]. OMRI, also known as Proton Electron Double Resonance Imaging (PEDRI), is a hyperpolarized MRI method and couples the advantages of MRI for spatial resolution with the specificity of EPR [10,13]. The high contrast enhancement in OMRI induced by dynamic nuclear polarization (DNP), where $\sim$110 times enhancement is achievable for ^{14}N-substituted nitroxides, confers superior contrast to noise ratio [11]. The relative merits and limitations of these three imaging modalities for nitroxides were examined and the estimated redox status information was found to be similar [8].

* Corresponding author. Fax: +1 301 480 2238.
E-mail address: matsumos@mail.nih.gov (S. Matsumoto).
[1] F. Hyodo and S. Matsumoto contributed equally to this work.

1090-7807/$ - see front matter © 2009 Published by Elsevier Inc.
doi:10.1016/j.jmr.2008.12.018

EPR imaging can be implemented using two different modes of signal detection namely the CW-EPR and the pulsed EPR [15]. Major advantages of pulsed EPR, which also known as time-domain EPR or Fourier transformed EPR, over the conventional CW-EPR are its rapid data acquisition and the lack of influence from subject motion during signal acquisition, while avoiding artifacts associated with modulation or RF power saturation [16]. In both cases, initially, image formation was achieved by the collection of projections under static magnetic field gradients and the reconstruction from projections using filtered back-projection methods. Though the time-domain EPR approach has similarities with the signal collection in MRI, the Fourier imaging methods used in MRI by switching gradients cannot be used since the gradient settling times are longer than the T_2 of many paramagnetic species. Recently, alternative Fourier imaging approach called single point imaging (SPI) has been implemented in time-domain EPR using static field gradients [17,18]. This approach forms images using pure phase encoding gradients and Fourier reconstruction. The feasibility of time-domain EPR imaging in *in vivo* applications has been demonstrated using trityl radicals which have long T_2s in the order of several microseconds. Though nitroxides have been imaged using time-domain EPR at X-band frequencies in spite of their shorter T_2s compared to trityl radicals, they were not detectable by time-domain EPR at 300 MHz till now because of the relatively longer spectrometer recovery time, which inversely correlates with the resonance frequency. With recent improvements in our spectrometer with respect to the spectrometer recovery time and sensitivity coupled with the fact that only a few points in the FID at a constant time interval need to be recorded with respect to their phase in the SPI, at the various phase encoding gradients, it became possible that nitroxides can be detected and imaged using pulsed EPR imaging at 300 MHz operating frequency.

In the present study, we applied the SPI technique to time-domain EPR imaging of nitroxides and, for the first time, successfully obtained well-resolved, distortion-free image of nitroxide distribution in mice. This method opens the capability of intracellular oxygen imaging for the first time.

2. Methods

2.1. Chemicals

^{15}N-PDT (4-oxo-2,2,6,6-tetramethyl piperidine-d$_{16}$-1-^{15}N-oxyl), ^{15}N-Tempol (4-hydroxyl-2,2,6,6-tetramethyl piperidine-1-^{15}N-oxyl), and ^{15}N-Tempamine (4-amino-2,2,6,6-tetramethyl piperidine-1-^{15}N-oxyl) were purchased from CDN Isotopes Inc. (Quebec, Canada). The triarylmethyl radical probe Oxo63 was obtained from GE Healthcare (Amersham, UK). To investigate concentration dependency of time-domain EPR signal of nitroxide, various concentrations (0.1–5 mM) of nitroxides and Oxo63 solutions in deuterium oxide were prepared under aerobic condition. Other materials used were of analytical grade.

A four-tube phantom, each tube (4.7 mm i.d.) containing 500 μL of 0.5 mM ^{15}N-PDT solution saturated with gas-mixtures 0%, 5%, 10%, 21% oxygen (nitrogen mixture) at room temperature for 15 min, was prepared to display the effect of T_2^* on the pulsed EPR image intensity from nitroxides.

2.2. Time-domain pulsed EPR scanner and SPI technique

Technical details of the time-domain EPR spectrometer operating at 300 MHz, data acquisition based on the single point imaging (SPI) modality, image reconstruction were described in the earlier reports [18,19]. Briefly, the SPI is a pure phase-encoding imaging technique. The free induction decay (FID) signals following the excitation pulse (80 ns, 80 W) were sampled using an analog–digital converter (200 mega samples/s). The repetition time (TR) of 5.5 μs corresponds to 180,000 excitations and acquisitions per second using 75° flip angle. For the FIDs collection, 1 mM solutions of three nitroxides and Oxo63 were measured with 100,000 averages. For 2D SPI imaging of the four-tube phantom, the FIDs were collected with a nested looping of the *X*, Z gradients and each time point in the FID undergoes phase modulation enabling 2D spatial encoding. Imaging parameters were as follows: field gradient = 0.8 Gauss/cm, number of gradient steps = 21 × 21, number of averages = 100,000.

Parallel coil resonators (25 mm i.d. with 25 mm long or 17 mm i.d. with 17 mm long) were used for the pulsed EPR imaging. The quality factor (*Q* value) of the coil has to be small in pulsed EPR in order to shorten the receiver recovery time, i.e., dead time and the *Q* value in the range 20–30 would be optimal for mouse imaging at 300 MHz in our pulsed EPR system. Image reconstruction was accomplished by using code written in MATLAB (Mathworks, Cambridge, MA).

2.3. Pulsed EPR imaging of nitroxide in mice

Female C3H Hen MTV mice were supplied by the Frederick Cancer Research Center, Animal Production (Frederick, MD, USA). The animals were received at 6 weeks of age and housed five per cage in a climate-controlled, circadian rhythm-adjusted room, and were allowed food and water ad libitum. Body weight measured before the experiments was 22–28 g. Mice were anesthetized by isoflurane (3% for induction and 1–2% for keeping anesthesia) in medical air (750 ml/min) and mounted prone on a special holder. A pressure transducer (SA Instruments, Inc., NY) was placed on the mouse to monitor and maintain steady breathing rate at 60 ± 15 per min. During EPR measurements, core body temperature of the mouse was monitored using a non-magnetic rectal temperature probe (FISO, Quebec, Canada) and maintained at 36.5 ± 1 C° with flow of warm air. A 30 G needle was cannulated into the tail vein and extended using polyethylene tubing (PE-10) for administration of nitroxide and Oxo63 solutions. ^{15}N-PDT (150 mM solution, 7.5 μL/g body weight) in phosphate buffered saline (PBS) was injected via tail vein, and then fast SPI scan was started. To confirm the position of kidneys, a bolus (10 μL/g body weight of 75 mM solution) of Oxo63, which is well known to accumulate into kidney, was intravenously injected into the same mouse after EPR signal of ^{15}N-PDT diminished beyond the detectable level, and imaging was started immediately thereafter. SPI data was collected with a field gradient of 1.0 Gauss/cm, 21 × 21 gradient steps, and 10,000 FIDs summed per gradient setting. The data-collection time per image was 27 s. The images were processed via Fourier reconstruction of a single time point at 800 ns from the trailing edge of the pulse.

To investigate the feasibility of oxygen mapping in tumor with pulsed EPR/nitroxide, Squamous Cell Carcinoma (SCC VII) cells were subcutaneously implanted in the right hind leg 10 days before the EPR measurements. Only tumor bearing leg was placed inside a smaller resonator (17 mm i.d. with 17 mm long). Immediately after ^{15}N-PDT injection, 3D-SPI imaging was performed with following parameters: maximum field gradient sets = 0.8, 0.92, 1.1 Gauss/cm, gradient steps = 11 × 11 × 11, number of averages = 7000, total acquisition time 2.5 min. Experiments were carried out in compliance with the *Guide for the Care and Use of Laboratory Animal Resources* (National Research Council, 1996) and approved by the National Cancer Institute Animal Care and Use Committee.

3. Results and discussion

Detecting the free induction decay signals from paramagnetic species in pulsed EPR demands instrumentation with nanosecond

time resolution, compared to millisecond–second order in MRI. Typically, an excitation pulse of ~100 ns creates the spin coherence which lasts for only 1–2 μs depending on the T_2 of the paramagnetic system. However, a significant portion of the FID is lost during the spectrometer recovery time which is typically 300–500 ns. While trityl radicals have FIDs which last longer than 1–2 μs, nitroxides with larger line widths have shorter FIDs with T_2 values in the range of 300–400 ns [21]. Additionally, only 1/3 of the ^{14}N-substituted nitroxides are typically probed as a result of their spectral multiplicity (triplet spectra) compared the trityl radicals imposing additional constraints on the sensitivity. Therefore, for a given resonator and input power, the resonator recovery, which is the major determinant in the spectrometer recovery time must be minimized which can be accomplished by reducing the *Q*. Reduction of resonator *Q* by over-coupling was found to be advantageous in terms of the achievable B_1 value and short dead times. Additional *Q* lowering is often achieved by resistive damping. The reduction of *Q* value of the parallel coil resonator with *Q* values in the range of 20–25 achieved by resistive damping and over-coupling, resulted in a dead time of ~300 ns for an input pulse of 80 ns width and 200 W power.

To examine the feasibility of detecting FIDs from nitroxides under the current spectrometer conditions, three different nitroxides were tested by time-domain EPR at 300 MHz and compared with the well known trityl radical, Oxo63 which has been used extensively *in vitro* and *in vivo* studies at this frequency range. Fig. 1 shows the FIDs of three different ^{15}N-substituted piperidine nitroxides (^{15}N-PDT, ^{15}N-Tempol, and ^{15}N-Tempamine) and Oxo63 in the absence of magnetic field gradients. It can be seen that, following the dead time, the FIDs of ^{15}N-Tempol and ^{15}N-Tempamine lasted for an additional 500 ns before disappearing in the noise level whereas the FID of Oxo63 lasted longer than 2 μs. The deuterated ^{15}N-PDT had a longer FID compared with other two nitroxides and its FID was detectable up to 1.5 μs. The T_2^* values calculated from the FIDs were 92, 94, 196, and 450 ns for ^{15}N-Tempamine, ^{15}N-Tempol, ^{15}N-PDT, and Oxo63, respectively. EPR signal remaining beyond the spectrometer dead time over total EPR signal were 3.9%, 4.2%, 21.7%, and 50.9% for ^{15}N-Tempamine, ^{15}N-Tempol, ^{15}N-PDT, and Oxo63, respectively. These signals lasted for shorter time intervals in imaging experiments where additional field gradients de phase the FIDs faster.

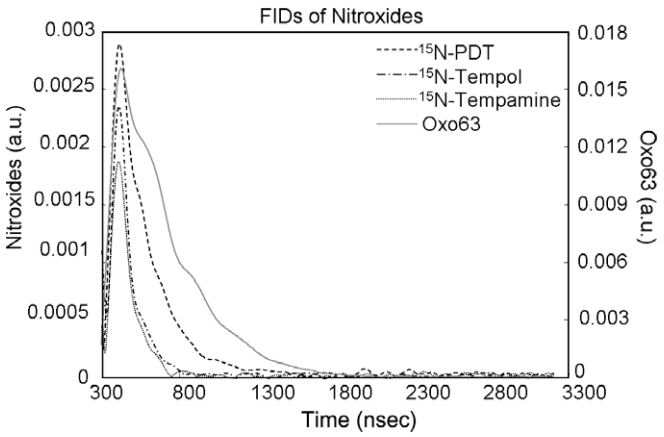

Fig. 1. FID signal of nitroxides by 300 MHz pulsed EPR spectroscopy. Pulsed EPR measurement of 1 mM solutions of three ^{15}N-substituted nitroxides (^{15}N-PDT, ^{15}N-Tempol, and ^{15}N-Tempamine) and Oxo63 was performed under medical air saturation. The FID of ^{15}N-PDT lasted beyond 1.5 μs after the excitation pulse, whereas FIDs of other two nitroxides ^{15}N-Tempol and ^{15}N-Tempamine disappeared under noise level within 1 μs. FID of Oxo63 could be detected longer than 2 μs after the excitation pulse.

The signal intensities of the various nitroxides and the trityl Oxo63 were monitored at different concentrations. The pulsed EPR signal intensity profile of nitroxides as a function of concentration was found to be biphasic and the shortening of T_2^* manifested at higher concentrations (Fig. 2A) mainly due to self-broadening. EPR signal intensity of nitroxides increased with concentrations, reached maximum at 1.5 mM for ^{15}N-PDT and 2.0 mM for ^{15}N-Tempol and ^{15}N-Tempamine, and started decreasing at higher concentrations. In contrast, EPR signal intensity of Oxo63 linearly increased till the concentration of 5 mM (Fig. 2B). The linear behavior exhibited by Oxo63 in this concentration range is consistent with its larger molecular size compared to nitroxides.

Based on the FID signal properties shown in Figs. 1 and 2, ^{15}N-PDT was selected for the *in vivo* imaging studies. It should be noted that prior studies have shown that the nitroxide ^{15}N-PDT is capable of permeating the cell membrane and therefore can localize both in intra- and extracellular locations unlike the trityl radical Oxo63, which because of the charge and substituents, is restricted to extracellular spaces. The pulsed EPR/SPI technique was applied to imaging the distribution of ^{15}N-PDT in mice after intravenous administration and the result is shown in Fig. 3A. The dosage of ^{15}N-PDT was optimized by estimating dilution in blood to provide maximum EPR signal intensity based on the concentration dependency as shown in Fig. 2 data, and delivered via tail vein and the images were obtained 20 s after injection. Significant distribution of ^{15}N-PDT was observed *in vivo* after intravenous injection. A series of 2D images taken as a function of time show that the intensity decreased rapidly with time, a phenomenon previously noticed with this class of compounds using CW-EPR and MRI [5,7,20]. After the signal from ^{15}N-PDT has diminished beyond the detection le-

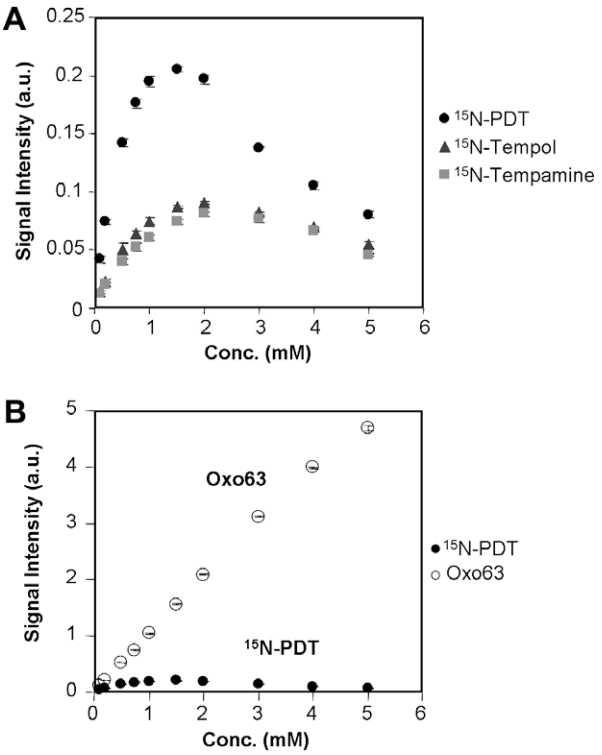

Fig. 2. Concentration dependency of pulsed EPR signal intensity of nitroxides. (A) Pulsed EPR signal intensity of ^{15}N-PDT reached maximum at 1.5 mM, whereas the other two nitroxides ^{15}N-Tempol and ^{15}N-Tempamine provided strongest signal at 2 mM. Biphasic manner of concentration dependency of pulsed EPR signal of nitroxides presumably due to self-EPR line broadening at higher concentrations, resulting in the shortening of T_2^*. (B) Pulsed EPR signal intensity of Oxo63 increased linearly at least till 5 mM.

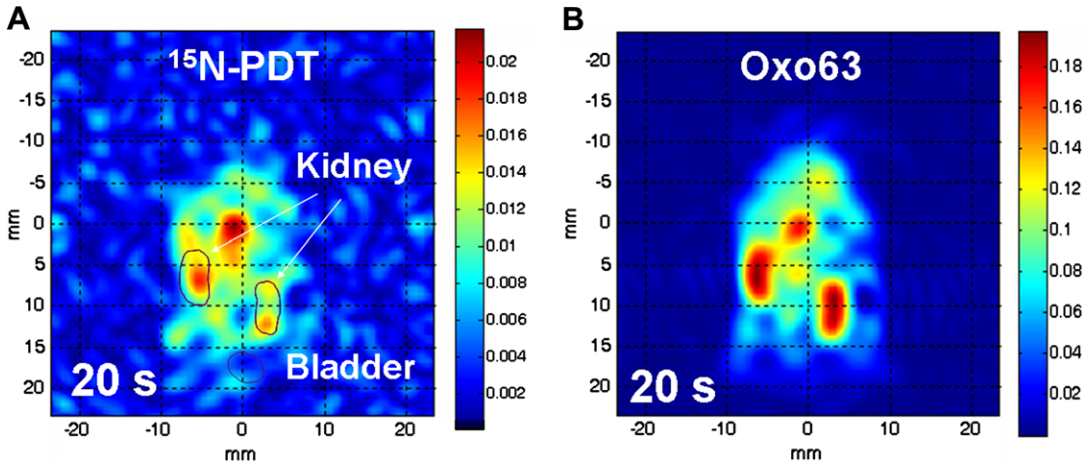

Fig. 3. Pulsed EPR imaging of nitroxide in mice. (A) The first pulsed EPR image of nitroxide distribution in mouse. (B) Pulsed EPR image of Oxo63 injected into the same mouse after ^{15}N-PDT signal disappeared.

vel, another set of image data were collected after injecting the cell-impermeable Oxo63. The EPR image of Oxo63 obtained 20 s after injection was similar to that of ^{15}N-PDT, and the accumulation of Oxo63 in the kidneys regions was observed.

Fig. 4A shows the SPI image of four-tube phantom containing ^{15}N-PDT solution equilibrated with gases containing different concentrations of oxygen and therefore imparting different line widths and consequent shortening of T_2^*. The image intensities from the four-tube phantom show that the EPR image intensity decreased along with increase in the oxygen concentration. This is explained in terms of the interaction of paramagnetic oxygen molecule to shorten the T_2^* of nitroxides, resulting in further signal loss within the dead time at higher oxygen concentrations. After demonstrating the capability to image the nitroxide ^{15}N-PDT at different levels of oxygen, the SPI/^{15}N-PDT system was applied to tumor oxygen imaging. The SCC tumor bearing leg was placed inside the smaller

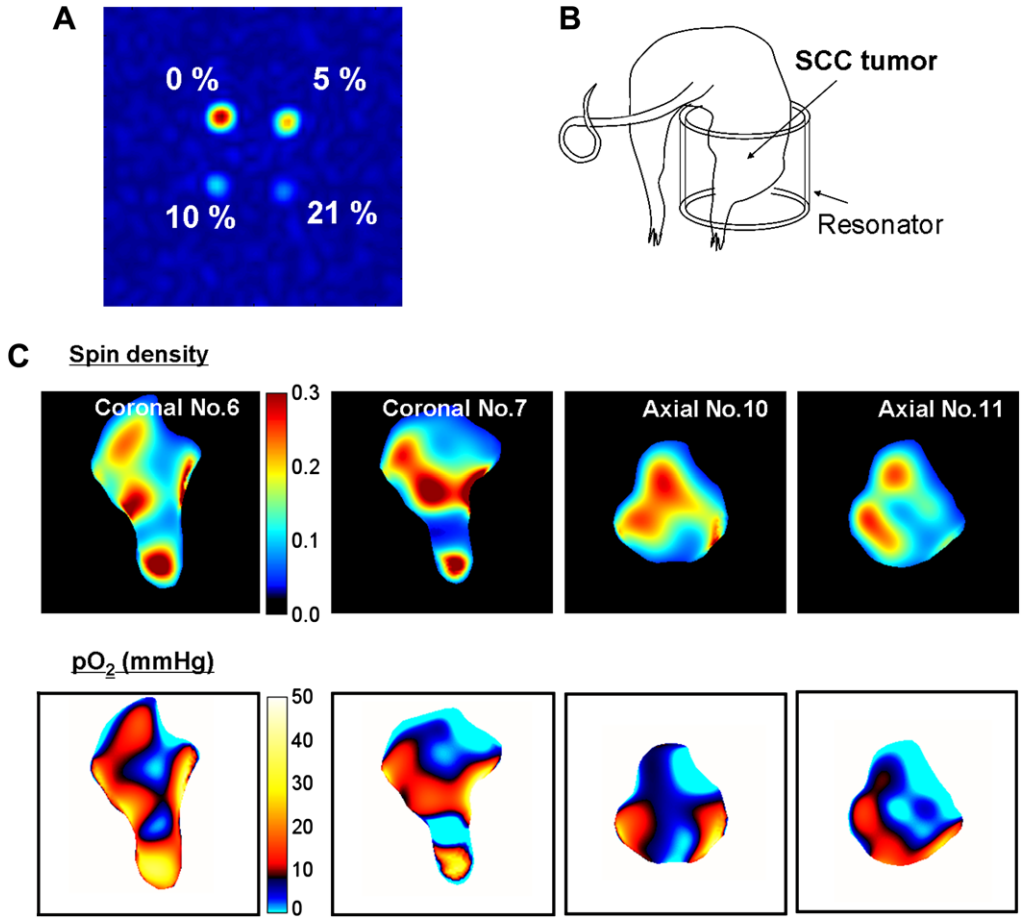

Fig. 4. 3D-pulsed EPR imaging of tumor oxygenation using nitroxide. (A) SPI image of four-tube phantom containing 0.5 mM ^{15}N-PDT solution saturated with 0%, 1%, 5%, 21% of oxygen gases. Pulsed EPR signal intensity decreased with increased oxygen concentrations because of T_2^* shortening effect of paramagnetic oxygen molecule. (B) Schematic illustration of tumor-implanted mouse setting in the smaller parallel coil resonator (17 mm i.d. with 17 mm long). (C) Coronal and axial slice views selected from 3D-SPI spin density map of ^{15}N-PDT in tumor bearing leg (top row) and corresponding oxygen images (bottom row) calculated from line width distribution of ^{15}N-PDT.

parallel coil resonator (Fig. 4B). FOV size was limited to the tumor bearing leg region to compress the 3D-SPI data acquisition time to be completed before the EPR signal of ^{15}N-PDT diminished below the noise level after intravenous injection ~2.5 min. Fig. 4C shows coronal and axial slice views selected from 3D-SPI spin density map of ^{15}N-PDT in tumor bearing leg and corresponding oxygen images calculated from line width distribution of ^{15}N-PDT. Significant hypoxic region (<10 mmHg) existed in the SCC tumor bearing mouse leg, which oxygen level was similar to or slightly lower than our previous results using Oxo63 as non-membrane permeable oxygen sensitive contrast agent in the same tumor model at the same timing [18].

This is the first report demonstrating the capability of detecting and imaging *in vivo* a cell-permeable nitroxide using pulsed EPR. With the capability of extracting oxygen dependent spectral line widths, this study points to the feasibility of probing intracellular concentrations of oxygen. Additionally, since nitroxide radicals have the flexibility of being targeted to specific intracellular locations by appropriate substituents, this study opens the possibility of using time-domain EPR to determine pO_2 in specific intracellular locations.

Acknowledgments

This work was supported by the Intramural Research Program, Center for Cancer Research, National Cancer Institute, NIH.

References

[1] J.B. Mitchell, A. Samuni, M.C. Krishna, W.G. DeGraff, M.S. Ahn, U. Samuni, A. Russo, Biologically active metal-independent superoxide dismutase mimics, Biochemistry 29 (1990) 2802–2807.
[2] B.P. Soule, F. Hyodo, K. Matsumoto, N.L. Simone, J.A. Cook, M.C. Krishna, J.B. Mitchell, The chemistry and biology of nitroxide compounds, Free Radic. Biol. Med. 42 (2007) 1632–1650.
[3] J.M. Metz, D. Smith, R. Mick, R. Lustig, J. Mitchell, M. Cherakuri, E. Glatstein, S.M. Hahn, A phase I study of topical Tempol for the prevention of alopecia induced by whole brain radiotherapy, Clin. Cancer Res. 10 (2004) 6411–6417.
[4] P. Kuppusamy, H. Li, G. Ilangovan, A.J. Cardounel, J.L. Zweier, K. Yamada, M.C. Krishna, J.B. Mitchell, Noninvasive imaging of tumor redox status and its modification by tissue glutathione levels, Cancer Res. 62 (2002) 307–312.
[5] H. Sato-Akaba, H. Fujii, H. Hirata, Development and testing of a CW-EPR apparatus for imaging of short-lifetime nitroxyl radicals in mouse head, J. Magn. Reson. 193 (2008) 191–198.
[6] S. Matsumoto, M. Nagai, K. Yamada, F. Hyodo, K. Yasukawa, M. Muraoka, H. Hirata, M. Ono, H. Utsumi, A composite resonator assembly suitable for EPR/NMR coregistration imaging, Conc. Magn. Reson. B Magn. Reson. Eng. 25B (2005) 1–11.
[7] F. Hyodo, K. Matsumoto, A. Matsumoto, J.B. Mitchell, M.C. Krishna, Probing the intracellular redox status of tumors with magnetic resonance imaging and redox-sensitive contrast agents, Cancer Res. 66 (2006) 9921–9928.
[8] F. Hyodo, R. Murugesan, K. Matsumoto, E. Hyodo, S. Subramanian, J.B. Mitchell, M.C. Krishna, Monitoring redox-sensitive paramagnetic contrast agent by EPRI, OMRI and MRI, J. Magn. Reson. 190 (2008) 105–112.
[9] K. Matsumoto, F. Hyodo, A. Matsumoto, A.P. Koretsky, A.L. Sowers, J.B. Mitchell, M.C. Krishna, High-resolution mapping of tumor redox status by magnetic resonance imaging using nitroxides as redox-sensitive contrast agents, Clin. Cancer Res. 12 (2006) 2455–2462.
[10] D.J. Lurie, J.M.S. Hutchison, L.H. Bell, I. Nicholson, D.M. Bussell, J.R. Mallard, Field-cycled proton–electron double-resonance imaging of free radicals in large aqueous samples, J. Magn. Reson. 84 (1989) 431–437.
[11] S. Matsumoto, K. Yamada, H. Hirata, K. Yasukawa, F. Hyodo, K. Ichikawa, H. Utsumi, Advantageous application of a surface coil to EPR irradiation in Overhauser-enhanced MRI, Magn. Reson. Med. 57 (2007) 806–811.
[12] H.M. Swartz, K. Chen, M. Pals, M. Sentjurc, P.D. Morse 2nd, Hypoxia-sensitive NMR contrast agents, Magn. Reson. Med. 3 (1986) 169–174.
[13] H. Utsumi, K. Yamada, K. Ichikawa, K. Sakai, Y. Kinoshita, S. Matsumoto, M. Nagai, Simultaneous molecular imaging of redox reactions monitored by Overhauser-enhanced MRI with ^{14}N- and ^{15}N-labeled nitroxyl radicals, Proc. Natl. Acad. Sci. USA 103 (2006) 1463–1468.
[14] F. Hyodo, K.H. Chuang, A.G. Goloshevsky, A. Sulima, G.L. Griffiths, J.B. Mitchell, A.P. Koretsky, M.C. Krishna, Brain redox imaging using blood–brain barrier-permeable nitroxide MRI contrast agent, J. Cereb. Blood Flow Metab. 28 (2008) 1165–1174.
[15] S. Subramanian, K. Matsumoto, J.B. Mitchell, M.C. Krishna, Radio frequency continuous-wave and time-domain EPR imaging and Overhauser-enhanced magnetic resonance imaging of small animals: instrumental developments and comparison of relative merits for functional imaging, NMR Biomed. 17 (2004) 263–294.
[16] S. Matsumoto, M.G. Espey, H. Utsumi, N. Devasahayam, K. Matsumoto, A. Matsumoto, H. Hirata, D.A. Wink, P. Kuppusamy, S. Subramanian, J.B. Mitchell, M.C. Krishna, Dynamic monitoring of localized tumor oxygenation changes using RF pulsed electron paramagnetic resonance in conscious mice, Magn. Reson. Med. 59 (2008) 619–625.
[17] S. Subramanian, N. Devasahayam, R. Murugesan, K. Yamada, J. Cook, A. Taube, J.B. Mitchell, J.A. Lohman, M.C. Krishna, Single-point (constant-time) imaging in radiofrequency Fourier transform electron paramagnetic resonance, Magn. Reson. Med. 48 (2002) 370–379.
[18] S. Matsumoto, F. Hyodo, S. Subramanian, N. Devasahayam, J. Munasinghe, E. Hyodo, C. Gadisetti, J.A. Cook, J.B. Mitchell, M.C. Krishna, Low-field paramagnetic resonance imaging of tumor oxygenation and glycolytic activity in mice, J. Clin. Invest. 118 (2008) 1965–1973.
[19] N. Devasahayam, S. Subramanian, R. Murugesan, F. Hyodo, K. Matsumoto, J.B. Mitchell, M.C. Krishna, Strategies for improved temporal and spectral resolution in in vivo oximetric imaging using time-domain EPR, Magn. Reson. Med. 57 (2007) 776–783.
[20] S. Matsumoto, I. Koshiishi, T. Inoguchi, H. Nawata, H. Utsumi, Confirmation of superoxide generation via xanthine oxidase in streptozotocin-induced diabetic mice, Free Radic. Res. 37 (2003) 767–772.
[21] M. Tseitlin, A. Dhami, R.W. Quine, G.A. Rinard, S.S. Eaton, G.R. Eaton, Electron spin T_2 of a nitroxyl radical at 250 MHz measured by rapid-scan EPR, Appl. Magn. Reson. 30 (2006) 651–656.